JOURNAL OF PROPULSION AND POWER
Vol. 17, No. 1, January–February 2001

# Scalar Variance Transport in the Turbulence Modeling of Propulsive Jets

N. Chidambaram,* S. M. Dash,† and D. C. Kenzakowski‡
*Combustion Research and Flow Technology, Inc., Dublin, Pennsylvania 18917*

**A variable turbulent Prandtl number model is applied to the prediction of laboratory jets with significant temperature variations. The model involves solving supplemental scalar equations for the temperature variance and its dissipation rate along with the $k$–$\varepsilon$ equations. The model is also applied to jets with variable composition with the aim of building a consolidated approach to model fluctuations of both temperature and species mass fraction. Comparisons are presented for subsonic jets for which scalar fluctuation measurements are available. The same coefficients are used for temperature/species variance and dissipation rate equations. Excellent agreement with data is obtained for round jets with respect to scalar fluctuation intensities and prediction of turbulent Prandtl/Schmidt numbers.**

## Nomenclature

| | | |
|---|---|---|
| $d_j$ | = | jet diameter |
| $k$ | = | turbulent kinetic energy |
| $k_T$ | = | temperature variance |
| $M$ | = | Mach number |
| $P_k$ | = | turbulent kinetic energy production term |
| $Pr_t$ | = | turbulent Prandtl number |
| $r$ | = | radial distance |
| $Sc_t$ | = | turbulent Schmidt number |
| $\tilde{T}$ | = | Favré-averaged temperature |
| $\tilde{u}_i$ | = | Favré-averaged velocity |
| $x$ | = | axial distance |
| $\alpha_t$ | = | eddy heat diffusivity |
| $\varepsilon$ | = | turbulent dissipation rate |
| $\varepsilon_T$ | = | temperature variance dissipation rate |
| $\mu$ | = | laminar viscosity |
| $\mu_t$ | = | turbulent viscosity |
| $\nu_t$ | = | eddy kinematic viscosity |
| $\bar{\rho}$ | = | mean density |

*Subscripts*

| | | |
|---|---|---|
| $e$ | = | external stream |
| $j$ | = | jet stream |
| $o$ | = | total conditions |
| $t$ | = | turbulent |

## Introduction

THE extension of jet turbulence model predictions to include scalar fluctuations has been motivated by varied concerns. For example, quantitative estimates about turbulent density fluctuations in jet plumes are essential for reliable aerooptical predictions. Information regarding the fluctuating behavior of species concentration and temperature is necessary to predict accurately reaction rates of chemically reacting turbulent flows. For complex flows, the prescription of a constant turbulent Prandtl number, as part of the standard heat-flux modeling approach (such as the gradient transport hypothesis), limits the generality of these models. The same is true for turbulent mass flux modeling using a constant Schmidt number. Because the turbulent Prandtl/Schmidt numbers can significantly alter the mean flow prediction, an ability to model the variation of these quantities is necessary.

Although these different application areas require the same prediction capability, common flowfield models have not been utilized and validated for different flow scenarios. In particular, specialized solution procedures emphasizing prediction of net outcome, namely, optical beam degradation, chemical heat release, and wall heat transfer, have been addressed. However, detailed comparisons of models with fundamental scalar fluctuation data have been minimal. The objective of the current work is to examine the available models and evolve a consolidated modeling approach to predict scalar variance and Prandtl/Schmidt numbers, with specific applicability to free-shear flows such as jets with density variations (due to temperature gradients or differing compositions). Within the traditional Reynolds-averaged Navier–Stokes methodology, the common approach to close the energy equation is to model the turbulent heat flux by a classical eddy-viscosity-type model. The eddy heat diffusivity is expressed in terms of the eddy kinematic viscosity and a turbulent Prandtl number ($\alpha_t = \nu_t/Pr_t$). Typically, a constant value is assumed for Prandtl number $Pr_t$ at this juncture. This is equivalent to an assumption of dynamic similarity between the turbulent heat and momentum transport. The commonly prescribed value for Prandtl number $Pr_t$ of approximately 0.9–1.0 is strictly valid only for homogeneous turbulent flowfields. Experiments and direct numerical simulations[1] (DNS) have indicated significant departures from the cited value even for classical flows such as jets and flat-plate boundary layers. A value of around 0.5 has been reported by Wygnanski and Fiedler[2] for a two-dimensional free-shear layer, and a value of 0.7 for axisymmetric round jets has been reported by Hinze.[3]

The most rigorous approach for the prediction of scalar variance is the utilization of full second-order closure models,[4] which is well beyond the realm of practical systems-oriented engineering applications. An equation for predicting scalar variance was introduced by Spalding,[5] which is popularly known as the $g$-equation. This model assumes a fixed ratio between the velocity and the scalar timescales to estimate the dissipation rate of the scalar variance. In other words, it assumes a fixed Prandtl number. Thus, this approach is inadequate to predict local variations in Prandtl number and is not general enough to handle different flow situations. Also, it would need low Reynolds number corrections to capture behavior near solid walls.

### Variable Prandtl Number Model

The turbulence model for scalar variance proposed by Nagano and Kim[6] uses the concept of eddy heat diffusivity. However, the

Received 4 February 1999; revision received 8 September 1999; accepted for publication 10 May 2000. 

*Research Scientist, P.O. Box 1150; currently Graduate Research Assistant, Institute fur Energietecknik, ETH-Zurich, Switzerland, CH-8092. Member AIAA.

†President and Chief Scientist, P.O. Box 1150. Associate Fellow AIAA.

‡Senior Research Scientist, P.O. Box 1150. Member AIAA.

specification of the turbulent Prandtl number is not required. The eddy heat diffusivity is expressed in terms of the turbulent kinetic energy, its dissipation rate, the temperature variance, and the temperature variance dissipation rate. This model has been modified for correct near-wall asymptotic behavior[7] and extended for compressible flows.[8] The model has been verified to capture consistently the features of flows such as flat-plate boundary layers and fully developed channel flow through comparisons with measurements and DNS data.

The validity of this model for high Reynolds number free shear flows, however, has not been established. The aim of the current work is to adapt and validate the model for hot jets and for jets with variable composition. The results will be compared to experiments, where scalar fluctuation measurements are available, by Panchapakesan and Lumley,[9] Lockwood and Moneib,[10] and Gaj and Rose.[11]

The set of temperature variance model coefficients used by Sommer et al.[8] for their pipe flow calculations was used for the axisymmetric jets, in this study, with only a slight change. The $k$–$\epsilon$ model coefficients for the axisymmetric jet calculations were the traditional values of Jones and Launder.[12]

### Outline

The following section describes the high Reynolds number scalar transport equations utilized. Comparison of simulation results with laboratory data for heated jets and for variable-composition jets is presented in the next section. A summary of the study is presented at the end.

## Governing Equation

The compressible Favré-averaged Navier–Stokes equations are solved for the mean flow quantities. Equations for the turbulent kinetic energy and its dissipation rate and for the temperature variance and its dissipation rate are also solved along with the Navier–Stokes equations in a coupled manner.

### Turbulent Kinetic Energy and Dissipation Rate Equations

The $k$–$\varepsilon$ model equations used are given as follows:

$$\frac{\partial \bar{\rho} k}{\partial t} + \frac{\partial \bar{\rho}\tilde{u}_j k}{\partial x_j} = \frac{\partial}{\partial x_j}\left[\left(\mu + \frac{\mu_t}{\sigma_k}\right)\frac{\partial k}{\partial x_j}\right] + \mu_t\left(\frac{\partial \tilde{u}_i}{\partial x_j}\right)^2 - \bar{\rho}\varepsilon \quad (1)$$

$$\frac{\partial \bar{\rho}\varepsilon}{\partial t} + \frac{\partial \bar{\rho}\tilde{u}_j k}{\partial x_j} = \frac{\partial}{\partial x_j}\left[\left(\mu + \frac{\mu_t}{\sigma_\varepsilon}\right)\frac{\partial \varepsilon}{\partial x_j}\right] + \frac{\varepsilon}{k}\left[C_{\varepsilon_1}\mu_t\left(\frac{\partial \tilde{u}_i}{\partial x_j}\right)^2 - C_{\varepsilon_2}\bar{\rho}\varepsilon + C_{\varepsilon_3}\bar{\rho}\varepsilon\chi\right] \quad (2)$$

where for round jets

$$\chi = \frac{1}{4}\left(\frac{k}{\varepsilon}\right)\left(\frac{\partial \tilde{u}}{\partial x} - \frac{\partial \tilde{v}}{\partial r}\right)\frac{v}{r} \quad (3)$$

The turbulent viscosity is given by

$$\mu_t = \bar{\rho} C_\mu k^2 \big/ \varepsilon \quad (4)$$

The values used for the model constants are as follows: $C_{\varepsilon 1} = 1.43$, $C_{\varepsilon 2} = 1.92$, $C_{\varepsilon 3} = 0.79$, $\sigma_k = 1.0$ and 1.45, and $C_\mu = 0.09$. For the axisymmetric jets, an additional vortex-stretching term[13] is also included, as represented by the last term in Eq. (2).

### Temperature Variance and Dissipation Rate Equations

The equations governing the transport of the temperature variance and its dissipation rate defined as

$$\varepsilon_t = \alpha \overline{\frac{\partial t''}{\partial x_k}\frac{\partial t''}{\partial x_k}} \quad (5)$$

are given as[8]

$$\frac{\partial \bar{\rho} k_t}{\partial t} + \frac{\partial \bar{\rho}\tilde{u}_j k_t}{\partial x_j} = \frac{\partial}{\partial x_j}\left[\bar{\rho}\left(\alpha + \frac{\alpha_t}{\sigma_{k_t}}\right)\frac{\partial k}{\partial x_j}\right] + 2\bar{\rho}\alpha_t\left(\frac{\partial \tilde{T}}{\partial x_j}\right)^2 - 2\bar{\rho}\varepsilon_t \quad (6)$$

$$\frac{\partial \bar{\rho}\varepsilon_t}{\partial t} + \frac{\partial \bar{\rho}\tilde{u}_j \varepsilon_t}{\partial x_j} = \frac{\partial}{\partial x_j}\left[\bar{\rho}\left(\alpha + \frac{\alpha_t}{\sigma_{\varepsilon_t}}\right)\frac{\partial \varepsilon_t}{\partial x_j}\right] + \left(C_{p_1}\frac{\varepsilon_t}{k_t} + C_{p_2}\frac{\varepsilon}{k}\right)\bar{\rho}\alpha_t\left(\frac{\partial \tilde{T}}{\partial x_j}\right)^2 + C_{p_3}\frac{\varepsilon_t}{k_t}P \quad (7)$$

where the operator ~ denotes Favré-averaged quantities. The same equation closure coefficients were used to model species fluctuations (concentration, total temperature) by substituting the corresponding species quantities in the place of temperature.

The values used for the constants are as follows: $C_{p_1} = 2.0$, $C_{p_2} = 0.0$, $C_{p_3} = 0.72$, $\sigma_{k_t} = 1.0$, and $\sigma_{\varepsilon_t} = 1.0$.

### Variable Prandtl Number

The attempt in this procedure is to model the turbulent heat diffusivity as a function of $k$, $\varepsilon$, $k_t$, and $\varepsilon_t$. A simple dimensional analysis shows that the resulting functional dependency can be written in terms of two nondimensional quantities:

$$\pi_1 = \frac{\alpha_t \varepsilon_t}{k k_t}, \qquad \pi_2 = \frac{k \varepsilon_t}{\varepsilon k_t} \quad (8)$$

It can be seen that $\pi_2$ is nothing but the ratio of the mechanical, $\tau_u$, to the thermal, $\tau_t$, turbulent timescales. As a result, the turbulent heat diffusivity can be written as

$$\alpha_t = (k k_t/\varepsilon_t) F(k\varepsilon_t/\varepsilon k_t) \quad (9)$$

Different ways of choosing the function $F$ are possible. By the assuming of a mixed timescale defined by $\sqrt{(\tau_u \tau_t)}$ for the diffusion of energy,[6] $\alpha_t$ can be written as

$$\alpha_t = C_\lambda k \sqrt{(k/\varepsilon)(k_t/\varepsilon_t)} \quad (10)$$

where $C_\lambda$ is a model constant (=0.14). This implies that

$$F = [(k/\varepsilon)(\varepsilon_t/k_t)]^{\frac{1}{2}} \quad (11)$$

The turbulent Prandtl number in turn can be expressed as

$$Pr_t = (C_\mu/C_\lambda)[(k/\varepsilon)(\varepsilon_t/k_t)]^{\frac{1}{2}} \quad (12)$$

The value of the model constant $C_\lambda$ used here differs slightly from that used by Sommer et al.[8] to predict better the turbulent Prandtl number for the axisymmetric jets.

### Numerical Formulations

The balanced pressure jet flow computations were performed using a parabolic space-marching algorithm[14] with 100 grid points spanning the jet width. Computations were performed with 20, 40, 60, and 80 points to confirm grid convergence. The $k_t$–$\varepsilon_t$ equations were also incorporated into the CRAFT Navier–Stokes code to confirm the validity of the parabolic assumptions. The CRAFT code is a finite-volume structured-grid solver with implicit time stepping, Roe's flux difference splitting, and total variation diminishing flux limiters. The Navier–Stokes equations are solved in a fully coupled manner using an alternating direction implicit method. The $k$–$\varepsilon$ and the $k_t$–$\varepsilon_t$ equations are solved fully coupled resulting in a $9 \times 9$ block tridiagonal matrix. The source terms are linearized and treated implicitly, and the diffusion coefficients including the turbulent diffusivities are lagged in time. Details of the numerical implementation can be found in the work by Sinha et al.[15]

## Axisymmetric Jet Computations

Because the jets considered have significant density differences, it is important to restrict the comparison to the nonbuoyant region of the jet development because the effect of buoyancy is not being modeled. By the use of the nondimensionalization advocated by Chen and Rodi,[16] a jet can be approximately divided into three regions, namely, the nonbuoyant jet region, the intermediate region, and the buoyant plume region.[9] The nondimensional length obtained from dimensional analysis is $x_l = F^{-1/2}\omega^{1/4}(x/d_j)$, where $F$ is the Froude number given as $F = U_j^2\rho_j/(\rho_e - \rho_j)gd_j$, where $\omega = \rho_e/\rho_j$. The points $x_1 = 0.5$ and $x_1 = 5$ were identified to delineate the three regions. All of the computations in the present study were made in the nonbuoyant jet region only. For all of the jet calculations, the computational domain extended up to an $x/d_j$ of 50.

### Heated Jet Comparisons

The heated axisymmetric jet of Lockwood and Moneib[10] was used to compare the performance of the scalar fluctuation model. In their experiment, a jet of heated air emerged from a vertical injector pipe of diameter 19.3 mm. The Mach number of the jet, $M_j$, was 0.24, and the total temperature $T_{oj}$ was approximately 548 K (Ref. 11). Fully developed turbulent pipe flow conditions would be expected

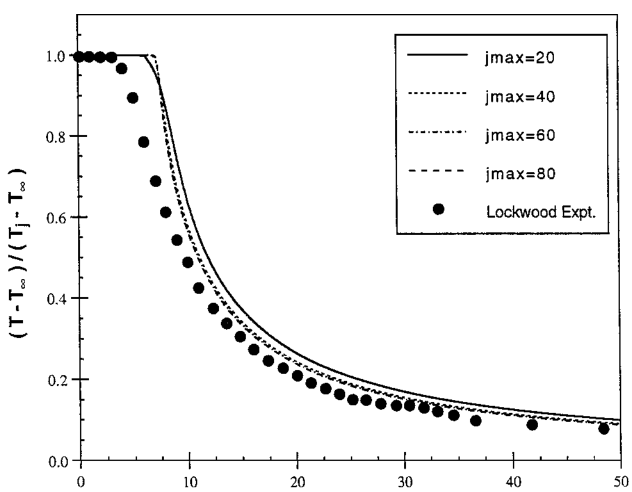


**Fig. 1 Centerline temperature decay: predictions vs Lockwood and Moneib[10] data.**

to prevail at the jet exit but were not available. Axial and radial variations of the mean and rms temperatures were compared and found to be in good agreement.

The Lockwood and Moneib[10] experiment was also repeated (with a convergent nozzle and 32.6 mm diameter) by Gaj and Rose,[11] along with two sets of sensitivity studies to explore the changes in the turbulent flow at a fixed position in the flow ($x/d_j = 20$) resulting from variations in $T_{oj}$ while holding $M_j$ fixed, and variations in $M_j$ while holding $T_{oj}$ fixed. Measurements for a high-speed jet with $M_j = 0.85$ and $T_{oj} = 578$ K into still air were also obtained. Comparisons with these experiments and trends are presented and are found to be quite good.

Figure 1 shows the decay of the mean temperature along the jet axis. Figure 1 shows a grid sensitivity study indicating that 20 points are inadequate but that 40 or more points provide grid-resolved results. The rate of decay shows good agreement between $10 < x/d_j < 50$. Differences observed near the jet exit are attributed to the difference in the initial conditions used. Top-hat profiles were used for the mean quantities with nominal values of turbulence intensity because the aim was to compare the asymptotic behavior. Earlier studies by the authors have shown that specification of approximate fully developed pipe flow profiles at the jet exit plane provided very good agreement to the spatial development.[17] Figure 2 exhibits predicted mean temperature contours for this case that show the overall extent of the thermal jet. Figure 3 shows grid sensitivity to the turbulent kinetic energy, again indicating that use of 40 or more points provides grid-converged results.

The temperature fluctuation intensity along the axis is shown in Fig. 4. The intensity is seen to asymptote to a value of 0.2, which is close to that observed in the experiment. A sudden increase in the intensity is observed as the mixing hits the axis as opposed to a gradual increase in the case of the experiment. This can be traced to the jet exit conditions, and this behavior has also been reported in other heated jet experiments where the jet exit profiles were not fully developed.[10] The results from the $M_j = 0.85$ case for total temperature fluctuation intensity are presented in Fig. 4.

Figure 5 shows the radial distribution of the temperature fluctuation intensity at different axial stations. The distinct off-axis peak is captured correctly. The radial variation of the turbulent Prandtl number is presented in Fig. 6. The model is successful in predicting the accepted value of 0.7 across the jet cross section.

The sensitivity of the temperature fluctuation to changes in $T_{oj}$ at $x/d_j = 20$ for $M_j = 0.85$ jet is shown in Fig. 7. The trend is captured correctly, although the values are a little higher due to different core lengths from the experiment.[11] Figure 8 shows the sensitivity to changes in $M_j$ at the same axial location. Again a good agreement with the trend is observed.

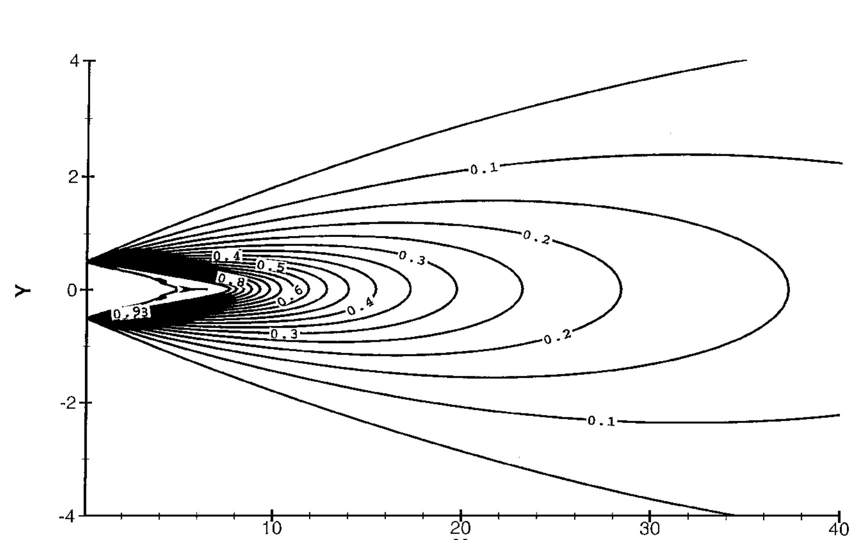


**Fig. 2 Predicted mean temperature contours for Lockwood and Moneib[10] jet.**

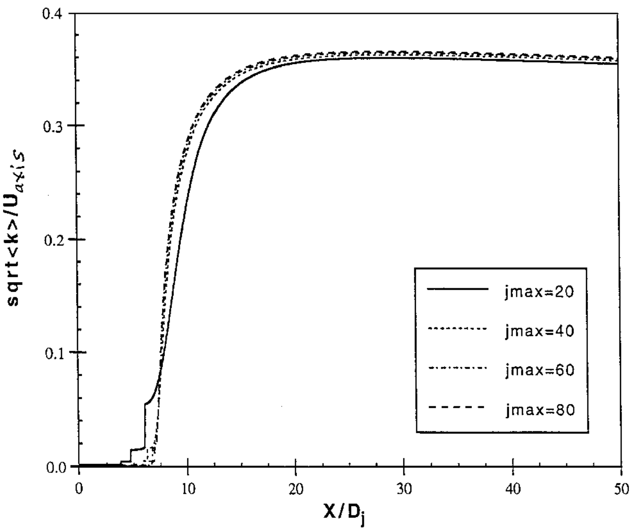


**Fig. 3 Variation of turbulent kinetic energy along the axis.**

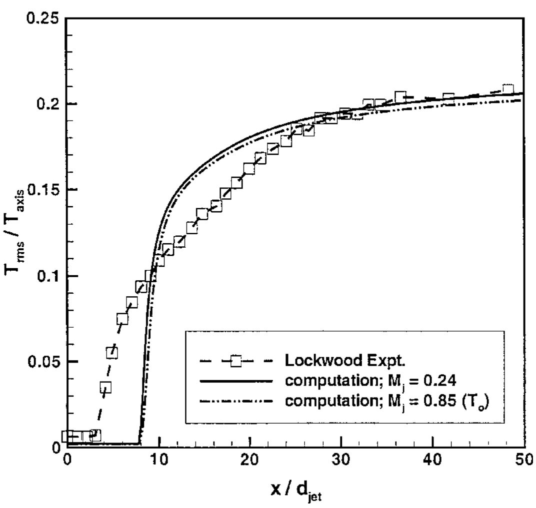


**Fig. 4 Variation of temperature fluctuation intensity along the axis.**

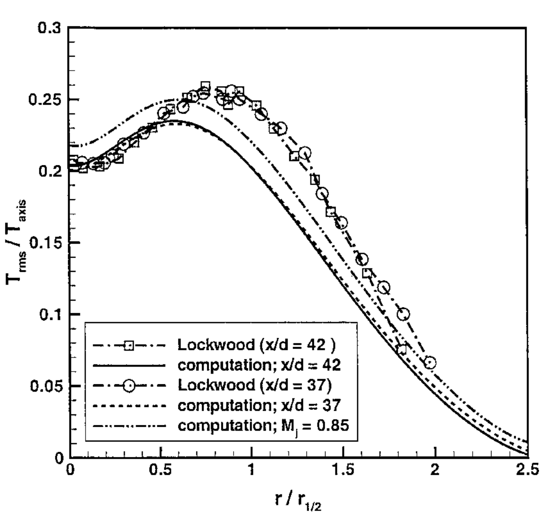


**Fig. 5 Radial variation of temperature fluctuation intensity.**

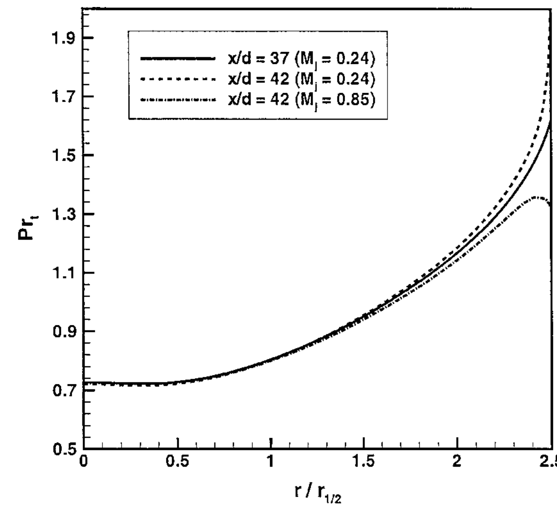


**Fig. 6 Radial variation of turbulent Prandtl number.**

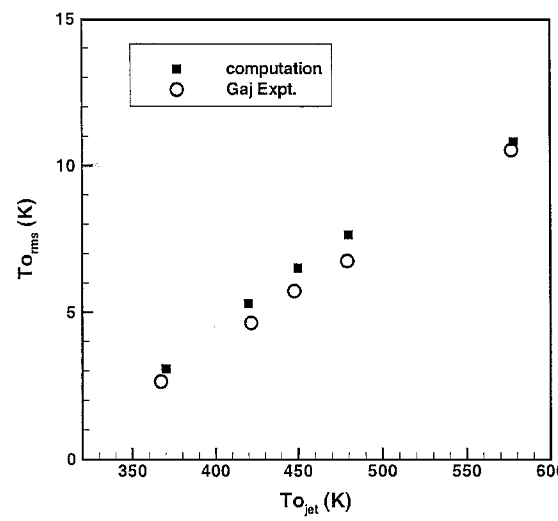


**Fig. 7 Change in rms total temperature with jet total temperature.**

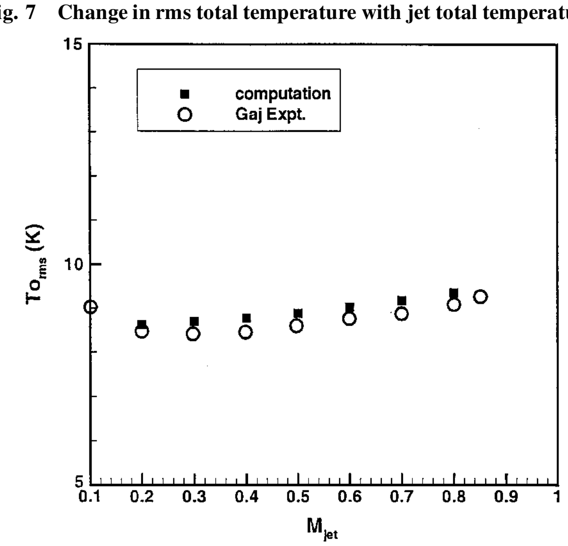


**Fig. 8 Change in rms total temperature with jet Mach number.**

## Helium Jet Comparisons

One of the aims of this study is to explore the feasibility of using the scalar fluctuation framework to predict fluctuation intensities of different scalars such as temperature, total temperature, and species concentration. Therefore, an attempt was made to use the model to predict concentration fluctuation for a helium jet into still air. The experiment by Panchapakesan and Lumley[9] was chosen for comparison. Unfortunately, their regime of measurement was beyond the nonbuoyant jet region, and direct comparisons are not possible. However, the results of experiments by Pitts[18] and Keagy and Weller[19] cited in Panchapakesan and Lumley's article were used to obtain quantitative comparisons.

Figure 9 shows the variation of the axial mean velocity and the mean helium concentration along the jet centerline. A linear fit to the concentration data of the form $1/F_c = K_c x/d$ gives a value for $K_c = 0.75$ compared to values of 0.69 and 0.73 reported by Pitts[18] and Panchapakesan and Lumley,[9] respectively. A similar fit to the

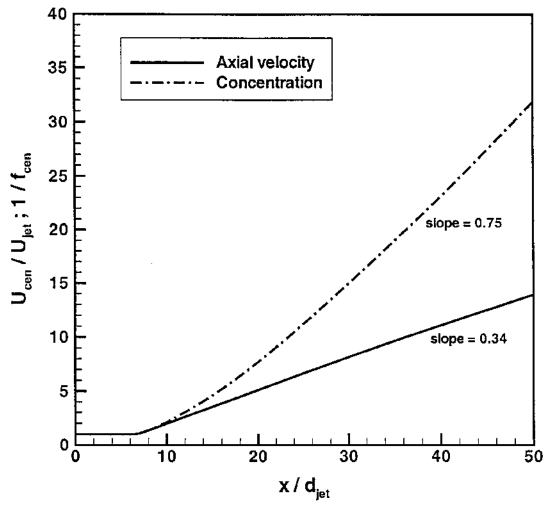


**Fig. 9 Axial variation of mean velocity and concentration for a helium jet.**

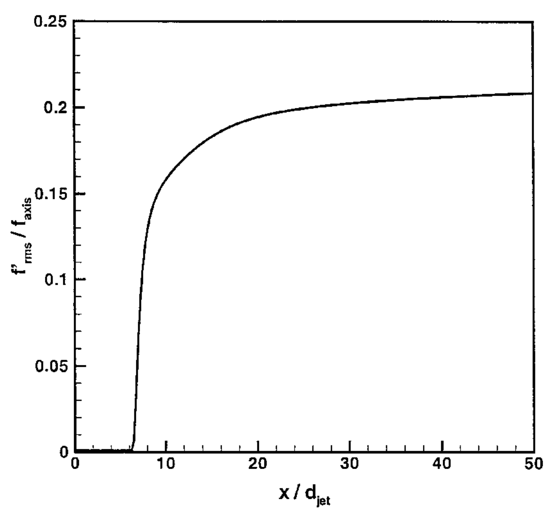


**Fig. 10 Axial variation of concentration fluctuation intensity.**

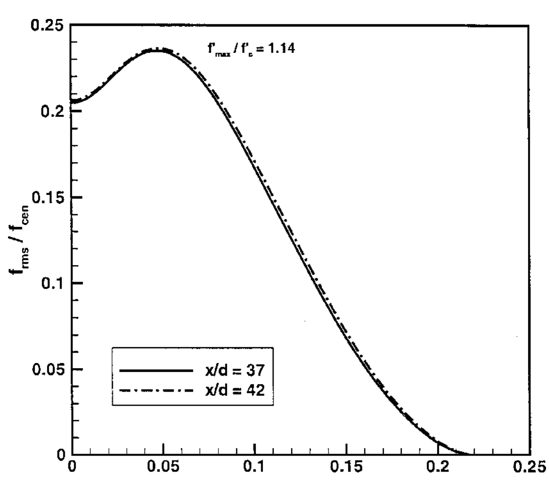


**Fig. 11 Radial variation of concentration fluctuation intensity.**

mean axial velocity gives a value of $K_c = 0.34$ as compared to 0.41 in the experiment.

Figure 10 shows the axial variation of the concentration fluctuation intensity. The intensity is observed to asymptote to a value of around 0.21. This is around the value of 0.23 measured by Pitts[18] and that measured by Panchapakesan and Lumley[9] of 0.21–0.22. Figure 11 shows the radial variation of the fluctuation intensity. The off-axis peak is captured with the ratio $f'_{max}/f'_c = 1.14$, and the position of the maximum $\eta_{max} = 0.05$. The variation of Schmidt number across the jet cross section is shown in Fig. 12. A value of 0.74 is predicted at the axis.

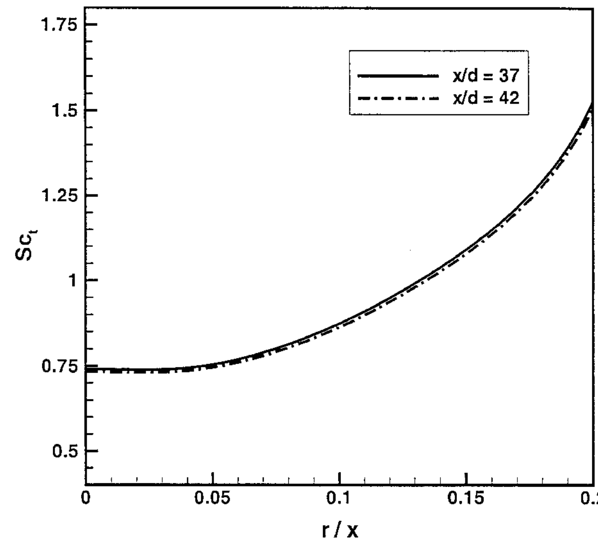


**Fig. 12 Variation of turbulent Schmidt number.**

## Summary

The variable Prandtl number model was validated for use to predict temperature variance for jets with significant density variations. The same model was used to predict variance of other scalars such as concentration and total temperature. Good agreement was obtained with available experiments. The model predicts the accepted value of 0.7 for the turbulent Prandtl and Schmidt numbers for axisymmetric jets. Further study will involve testing of the model for planar free shear flows, namely, two-dimensional shear layers and planar jets. Extensions to the model to account for compressibility effects in high-speed flows and to operate with advanced turbulent models are envisioned.

## References

[1]Madavan, N. K., and Rai, M. M., "Direct Numerical Simulation of Boundary Layer Transition on a Heated Flat Plate with Elevated Freestream Turbulence," AIAA Paper 95-0771, Jan. 1995.

[2]Wygnanski, I., and Fiedler, H. E., "The Two-Dimensional Mixing Region," *Journal of Fluid Mechanics*, Vol. 41, No. 2, 1970, p. 327.

[3]Hinze, J. O., *Turbulence*, McGraw-Hill, New York, 1975, pp. 534–545.

[4]Wallit, L., and Ratliff, A. W., "Evaluation of the $k$–$\varepsilon$ and Second Order Closure Turbulence Models for Determination of Density Fluctuations in Hypersonic Shear Layers," AIAA Paper 93-2680, June 1993.

[5]Spalding, D. B., "Concentration Fluctuations in a Round Turbulent Free Jet," *Chemical Engineering Science*, Vol. 26, 1971, pp. 95–107.

[6]Nagano, Y., and Kim, C., "A Two-Equation Model for Heat Transport in Wall Turbulent Shear Flows," *Journal of Heat Transfer*, Vol. 110, Aug. 1988, pp. 583–589.

[7]Sommer, T. P., So, R. M. C., and Lai, Y. G., "A Near-Wall Two-Equation Model for Turbulent Heat Fluxes," *International Journal of Heat and Mass Transfer*, Vol. 35, No. 12, 1992, pp. 3375–3387.

[8]Sommer, T. P., So, R. M. C., and Zhang, H. S., "Near-Wall Variable-Prandtl-Number Turbulence Model for Compressible Flows," *AIAA Journal*, Vol. 31, No. 1, 1993, pp. 27–35.

[9]Panchapakesan, N. R., and Lumley, J. L., "Turbulence Measurements in Axisymmetric Jets of Air and Helium," *Journal of Fluid Mechanics*, Vol. 246, July 1993, pp. 197–247.

[10]Lockwood, F. C., and Moneib, H. A., "Fluctuating Temperature Measurements in a Heated Round Free Jet," *Combustion Science and Technology*, Vol. 22, No. 1-2, 1980, pp. 63–81.

[11]Gaj, R. A., and Rose, W. C., "Turbulence Measurements in a Heated High-Speed Axisymmetric Laboratory Jet," Pacific-Sierra Research Corp., Rept. 2480, Santa Monica, CA, Sept. 1994.

[12]Jones, W. P., and Launder, B. E., "The Prediction of Laminarization with a Two Equation Model of Turbulence," *International Journal of Heat and Mass Transfer*, Vol. 15, 1972, pp. 301–314.

[13]Pope, S. B., "An Explanation of the Turbulent Roundjet/Planejet Anomaly," *AIAA Journal*, Vol. 16, No. 3, 1978, pp. 279–281.

[14]Dash, S. M., Sinha, N., and York, B. J., "Implicit/Explicit Analysis of Interactive Phenomena in Supersonic, Chemically Reacting, Mixing and Boundary Layer Problems," AIAA Paper 85-1717, July 1985.

[15]Sinha, N., Hosangadi, A., and Dash, S. M., "The CRAFT NS Code and Preliminary Applications to Steady/Unsteady Reacting, Multi-Phase Jet/Plume Flowfield Problems," CPIA Publ. 568, Chemical Propulsion Information Agency, Laurel, MD, May 1991, pp. 203–226.

[16]Chen, C. J., and Rodi, W., "Vertical Turbulent Buoyant Jets—A Review of Experimental Data," Vol. HMT-4, Pergamon, Oxford, England, U.K., 1980.

[17]Dash, S. M., and Kenzakowski, D. C, "Turbulence Interactions Program Final Report Volume III: CFD Comparisons and Data Comparisons," Combustion Research and Flow Technology Inc., CRAFTR-6/95.003, Dublin, PA, 1995.

[18]Pitts, W. M., "Effects of Global Density and Reynolds Number Variations on Mixing in Turbulent, Axisymmetric Jets," National Bureau of Standards, NBSIR 86-3340, U.S. Dept. of Commerce, 1996.

[19]Keagy, W. R., and Weller, A. E., "A Study of Freely Expanding Inhomogeneous Jets," *Heat Transfer Fluid Mech Inst.*, Vol. 10, 1949, pp. 89–98.